N78-24062

ANALYTICAL DEVELOPMENTS FOR DEFINITION AND PREDICTION OF USB NOISE*

N. N. Reddy and C. K. W. Tam**
Lockheed-Georgia Company

SUMMARY

A systematic acoustic data base and associated flow data were used in identifying the noise generating mechanisms of upper surface blown flap configurations of short takeoff and landing aircraft. Theory is developed for the radiated sound field of the highly sheared flow of the trailing edge wake. An empirical method is also developed using extensive experimental data and physical reasonings to predict the noise levels.

INTRODUCTION

It is clear from previous investigations (refs. 1-3) that most of the far-field sound field of upper surface blown flap configurations of STOL aircraft is from the interaction of turbulent jet flow with wing and flap surfaces. Analysis of the sound produced by interaction between turbulent flow and rigid surfaces, starting from the first principles, is very difficult if not impossible. Therefore, it is necessary to rely upon experimental data. Using the flow and noise data generated from a systematic experimental program at Lockheed under contract to NASA-Langley, the noise characteristics of USB are defined. The important source from a community standpoint is identified as the noise generated in the vicinity of the trailing edge. Therefore, theoretical analysis is performed for the sound field produced by the flow in the trailing edge wake, where the velocity gradient and turbulence intensity are large, using experimentally obtained flow characteristics. An empirical method is also developed using the noise data base and physical arguments which may be used to predict the noise levels — at least until the theory is developed further. addition, a brief discussion of the effect of aircraft motion and noise suppression is presented.

16

*Research performed under NASA Contract NAS1-13870.
**Professor, Department of Mathematics, Florida State University, Tallahassee, Florida.

240

PAGE INTENTIONALLY BLANK

NOISE MECHANISMS

The aerodynamic noise produced by the upper surface blown flap (USB) system may be summarized and idealized as the noise generated by the interference of a turbulent jet with finite rigid surfaces. Based upon the experimental and theoretical investigations, it is hypothesized that the propulsive lift related sound may be attributed to eight possible sources which differ in their geometric location and noise generation and propagation mechanisms. These sources are illustrated in figure 1.

Engine Internal Noise

Noise generated within the engine, which includes fan, compressor, and turbine noise, is known as internal noise. This propagates in the forward as well as in the aft directions. The forward-radiated noise is not peculiar to USB configurations, but most of the aft-radiated sound is shielded from the community by the wing and flap. This subject is really beyond the scope of this paper and thus will not be discussed in any detail.

Jet Mixing Noise

The jet flow prior to its impingement is defined as the USB jet mixing region. The noise generated in this region is called jet mixing noise. The fundamental flow mixing is modified by the presence of the rigid surface. Therefore, the noise generation process of flow mixing in this region may not be the same as free jet mixing without the presence of the wing. In the case of USB, however, this region of free jet mixing is close to the nozzle exit and above the wing. Therefore, most of this noise will be shielded from the community by the wing and flap as in the case of engine internal noise.

Jet Impingement Noise

When the jet is deflected onto the wing from an elevated position, as in the case of pylon-mounted engines, the jet exhaust flow impinges on the wing surface. This turbulent flow impinging on the surface generates additional noise generally known as "impingement noise." Even though the strength of this source could be significant (depending on the configuration), the radiated sound from this source below the wing for a typical aircraft configuration may be negligible because of its geometric location. In certain extreme cases, this noise may radiate toward the forward quadrant.

Wall Jet Boundary Layer Noise

The wall jet boundary layer on the wing and flap surface will have a high mean shear and can produce a high turbulence level, and noise is thus generated by the induced fluctuating pressures on the surface. The contribution of this

wall jet boundary layer noise to the community is very small because (1) the volume of turbulence of boundary layer is small compared to the volume of other noise-producing regions, and (2) the noise is generated above the wing and therefore shielded by the wing/flap.

Wall Jet Mixing Noise

The developed wall jet will be formed immediately after the impingement of the jet flow on the wing surface. The mixing of jet flow with the entrained air in this region results in fluctuating stresses similar to free jet mixing. The noise generated in this region is known as wall jet mixing noise. The introduction of curvature on the surface modifies the wall jet thickness and velocity decay rate and amplifies the turbulence levels in the flow. The contribution of sound from this source is primarily in the direction above the wing and possibly in the aft quadrant below the wing.

Trailing Edge Noise

Noise generated in the vicinity of the flap trailing edge is generally known as trailing edge noise. All the previous experiments and analyses indicate that the contribution of sound from this source, particularly in the direction below the wing, is dominating. However, there is no agreement among the various investigators about the noise-generating mechanism. For example, Hayden (ref. 4) has hypothesized that the turbulent flow leaving the surface at the trailing edge generates a strong dipole source with preferred axis perpendicular to the surface. Ffowcs Williams and Hall (ref. 5), on the other hand, analyzed the radiated sound field for quadrupole noise sources in the vicinity of the edge of a semi-infinite rigid surface. Both of these analyses gave essentially the same directivity and spectral distribution. However, closer examination of experimentally obtained, radiated sound field and flow-field data indicate that the trailing edge noise could be generated in the shear layer of the trailing edge wake. This will be discussed further under "Mathematical Model."

Wall Jet Roll-Up Noise

It is observed that the jet rolls up at the edges of the surface and grows as the axial distance from the nozzle increases. This roll-up phenomenon becomes stronger as the curvature increases and further amplifies as the aspect ratio of the nozzle decreases. The noise generated by this type of flow instability is known as wall jet roll-up noise. It appears that, for large aspect ratio nozzles or for the case where the jet flow spreads fairly well, the noise generated by roll-up is small. However, for small aspect ratio nozzles, this may not be negligible.

Flow Separation Noise

There are certain operational and geometrical configurations where the jet flow can separate before it reaches trailing edge. In fact, separation was observed in the wind tunnel experiments with forward speed for some cases where there is no separation during static tests. This phenomenon of separation obviously generates additional noise as discussed by Siddon (ref. 6). This separation noise could be significant in the aft quadrant, depending on the separation location.

In addition to the noise sources discussed so far, there may be acoustic feedback mechanisms which can result in large magnitudes of discrete frequency noise. Since it is observed that this type of noise is very sensitive to operational and geometric parameters, it is assumed that these conditions may be avoided with a careful design.

RADIATED SOUND FIELD

In order to identify the dominant noise source contributing in various directions, the spatial distribution of the one-third octave spectra is examined. Figure 2 illustrates the typical spectra in various directions in the flyover plane. It may be observed that, as the angle θ from the forward axis of the wing plane increases, the noise levels — particularly in the high-frequency range — increase. As we approach the direction above the flap surface (for $\theta > 150°$), the noise levels further increase and then start decreasing with the increase in θ. From these results and the results presented in the previous papers (refs. 7 and 8) and with the assumption that most of the noise generated upstream of trailing edge is shielded from radiating below by the wing and flap surfaces, it may be conjectured that the trailing edge noise is a dominant source from a community noise standpoint. In order to examine this hypothesis further, the sound pressure level spectra for different flap angles shown in figure 3 are studied. It may be observed that there are two peak sound levels at about 0.8 kHz and 2.0 kHz with a dip at 1.0 kHz. This type of spectral distribution is consistent with most of the tests, including tests at NASA (refs. 3 and 9). This observation led some investigators to conjecture that two sources, with low- and high-frequency dominance, contribute to the radiated sound in this direction. But closer examination of the experimental data indicates that the frequencies of these humps and dip are independent of flap angle, as shown in this figure, and they are also independent of jet velocity as shown in figure 4. It is suspected that the sound generated in the trailing edge wake and diffracted by the wing leading edge and rigid surfaces of the test rig, such as nozzle flange and the wing/flap end plates (as seen in one of the model descriptions of ref. 8), could cause the reinforcement and cancellation of radiated sound at certain frequencies. These possibilities are explored further experimentally by using sound absorbent material on several of these surfaces. The results are shown in figure 5. As can be seen, the humps and dip are eliminated in the frequency range of 500 to 2000 Hz by avoiding the surface diffraction. Therefore, it may be inferred that the spectral

distribution of radiated sound without diffraction is broad-band type at least in the low-frequency range up to 2000 Hz.

From these results, it is postulated that only the trailing edge is a dominant source contributing below the wing, and some of the other aeroacoustic sources discussed in the previous section — including the trailing edge noise — could contribute above the wing. Since the noise characteristics below the wing are more pertinent from community noise standpoint, further analysis is made on the trailing edge noise source.

MATHEMATICAL MODEL

A closer examination of the experimentally measured sound and flow field revealed that there was no clear-cut evidence to associate the trailing edge noise to either dipole model, as depicted by Hayden (ref. 4), or the diffracted quadrupole, as formulated by Ffowcs Williams and Hall (ref. 5). The typical flow characteristics just downstream of the trailing edge wake which are shown in figure 6 indicate that the velocity gradient and turbulence intensity are very large near the edge. In fact, it may be observed that the turbulence intensity is maximum where the velocity gradient is maximum. Experience tells us that the by-product of turbulence generation is noise generation or a noise source. Therefore, a mathematical model was developed for the turbulent mixing noise of the highly sheared trailing edge wake flow. In this model, the sheared flow downstream of the trailing edge is assumed to be locally two-dimensional and spatially homogeneous with respect to any plane parallel to the shear layer. These assumptions are justified experimentally, as discussed in reference 7. In addition, it is also assumed that the fluid within the shear layer is incompressible, which is reasonable for the flow velocity very much smaller than sonic velocity. With these assumptions and the equations of motion (Poisson's equation), the pressure fluctuations associated with turbulent mixing are found in terms of unsteady velocity components with the use of the Fourier transform. This result is then used to form the space-time near-field pressure cross-correlation function. Assuming only the shear components are important for radiated noise, these terms alone are retained.

This analysis illustrates that, for a practical upper surface blown flap configuration, the turbulent mixing in the vicinity of the trailing edge is a dominant noise source. The radiated noise is primarily a function of the flow parameters in the trailing edge wake. However, the typical streamwise space-time cross-correlation function of fluctuating velocities in the trailing edge wake, shown in figure 7, exhibit similar characteristics as in the shear layer close to the nozzle exit of the free jet. A function of the following form is derived as given by Maestrello (refs. 10 and 11):

$$R_w(\bar{x},\bar{y},z',z'',\tau) = G(z',z'')e^{\bar{x}/\lambda\delta} \sum_{i=1}^{n} \frac{\alpha_i A_i}{\alpha_i^2 + \left[\frac{\bar{U}}{U_c\delta}\right]^2 [(\bar{x} - U_c\tau)^2 + \beta^2\bar{y}^2]} \qquad (1)$$

where (see appendix for additional symbols)

$\bar{x} = \lvert x' - x'' \rvert$	streamwise (longitudinal) separation distance
$\bar{y} = \lvert y' - y'' \rvert$	spanwise separation distance
z', z''	lateral measurement locations
τ	delay time
λ	longitudinal decay rate of the cross-correlation function
δ	the shear layer thickness
U	maximum velocity in the trailing edge wake
U_c	eddy convection velocity
β	scale of anisotropy (ratio of longitudinal to the lateral length scales)
$G(z', z'')$	transverse correlation function of zero time delay
α_i and A_i	the empirical constants to describe the shape of the power spectrum of the fluctuating velocities

The far-field sound pressures were calculated by considering the fluctuating pressure components with supersonic phase velocity as given by Tam (ref. 12). The detailed discussion of the analysis of radiated sound from the trailing edge wake sheared layer of USB using experimentally obtained fluctuating velocity characteristics is presented in a paper to be presented in the AIAA aeroacoustics conference in July 1976 (ref. 13). The final expression for the radiated sound pressure per unit area of shear layer per unit solid angle in the direction ψ from the flow direction and per unit frequency at a frequency of ω, $D(\psi,\omega)$ is given as

$$\frac{D(\psi,\omega)}{\rho U^2 \delta} = \frac{\frac{U_c}{U}\left(\frac{\omega\delta}{U}\right)}{2\pi^2 \beta \lambda} M^3 \sin\psi \cdot \frac{\sum_{i=1}^{3} \left\{ \frac{A_i \alpha_i \nu_o \left(\alpha_i \frac{\omega\delta}{U}\right)}{\frac{1}{\lambda^2} + \left(\frac{\omega\delta}{U}\right)^2 \left(M\cos\psi - \frac{U}{U_c}\right)^2} \right\}}{\sum_{i=1}^{3} \frac{A_i}{\alpha_i}}$$

$$\cdot \left\{ \frac{1}{\bar{U}^4} \int_{-\delta}^{0} \int \frac{d\bar{U}}{dz'} \frac{d\bar{U}}{dz''} \cdot G(z', z'')\, dz' dz'' \right\} \qquad (2)$$

where

M is the flow Mach number based on ambient speed of sound

$K_0(x)$ is the zeroth order modified Bessel function

$d\bar{U}/dz'$ is the velocity gradient in the sheared layer.

The flow characteristics were measured using two single hot wires for a configuration shown in figure 8 in the mid-span just downstream of the trailing edge. A rectangular nozzle with aspect ratio of 8 and exit area of 20.26 square centimeters was used. The wing and flap consisted of 60° flap angle with 7.62 cm radius of curvature. The flow length, defined as the length between the nozzle exit to the trailing edge of the flap, was 21.8 cm. The following values were obtained from the hot-wire correlation and velocity and turbulence intensity measurements for maximum velocity, convection velocity, and length scales:

$$U = 74.4 \text{ m/s}$$

$$U_c = 67 \text{ m/s}; \qquad U_c/U = 0.9$$

$$L_x = 0.85 \text{ cm}$$

$$L_y = 0.35 \text{ cm} \qquad L_x/L_y = 2.4$$

$$\delta = 0.8 \text{ cm}$$

Shear layer thickness δ is defined as the height from 10% to 90% of maximum velocity.

A_i's and α_i's are determined using the measured auto correlation function shown in figure 9 as

$$A_1 = 0.7, \qquad A_2 = 6.3, \qquad A_3 = 3.0$$

$$\alpha_1 = 0.32, \qquad \alpha_2 = 1.4, \qquad \alpha_3 = 20.0$$

One-third octave band sound pressure levels are calculated using these values of flow properties in equation (2) in various directions at center frequencies of 400, 1600, and 6300 Hz. These results are compared with the measured radiated sound in figure 10. Comparison is also made in figure 11 between measured and calculated one-third octave band sound pressure level spectra in the direction of 10° to the flow. It may be observed from these two figures that there is a favorable agreement, particularly in the high-frequency region. The theoretical calculations may be improved if the turbulence properties are measured more precisely by considering the components of each direction. This may be accomplished with more sophisticated hot-wire system or laser velocimeter developed recently at Lockheed.

This analysis illustrates that, for a practical upper surface blown flap, the turbulent mixing in the vicinity of trailing edge is a dominant noise source. The radiated noise is primarily a function of the flow parameters in

the trailing edge wake. However, in order to estimate the effect of geometric and operational parameters on noise characteristics, it is necessary to establish the relationship between the trailing edge flow characteristics and the various parameters. But, to do so would require extensive experimental measurements which are not available at the present time. Therefore, using the systematic far-field sound measurements for various configurations and with the physical reasonings, an empirical method of USB noise-prediction method has been developed.

EMPIRICAL METHOD OF NOISE PREDICTION

In developing a noise-prediction program, an attempt is made to generalize the observations made in the extensive flow and acoustic data base and to incorporate them in the empirical model. Since the primary interest is in the direction below the wing, it is assumed that the dominant noise is from the trailing edge source. Therefore, the noise levels should be correlated with the gross parameters in the trailing edge wake such as velocity, turbulence, and jet thickness at the trailing edge. However, at the present state of the art, it is not possible to relate these trailing edge parameters to operational and geometric parameters. Thus, the empirical relations are derived using the readily available engine and wing/flap parameters. General variation of noise characteristics as a function of geometric and operational parameters is discussed briefly.

Nozzle Area and Shape

The radiated sound intensity is found to be directly proportional to the nozzle area. Generally, the noise levels increase as the aspect ratio decreases. For noise prediction, spectral shape is assumed independent of shape.

Nozzle Exit Velocity

The sound intensity is found to increase as the jet velocity increases; the velocity exponent varies from 5.0 to 7.5 depending on the direction as shown in figure 12. The frequency is directly proportional to the jet velocity.

Radius of Curvature

The magnitude and spectral characteristics are independent of radius of curvature, which means the sound intensity and spectral distribution do not depend on the sharpness of the flow turn provided that the flow was completely turned and attached to the complete longitudinal length of the flap surface without flow separation.

Flow Length

Flow length appears to be an important parameter. As the flow length increases, both the sound intensity and the frequency of the spectrum decrease. This is due to the reduction in velocity and perhaps due to increase in the jet thickness at the trailing edge.

Flap Angle

For a constant angle with respect to the flap (flow direction in the trailing edge wake), the sound intensity is independent of the flap angle. However, the peak frequency of the spectrum is reduced as the flap angle is increased. Again, this may be due to increase in the jet thickness as the flap angle increases.

An illustration of nondimensional spectral distribution derived from the data to develop the prediction procedure is given in figure 13. Here, it is assumed that the sound pressure varies as jet velocity raised to the power 7, and the nondimensional frequency is a function of flow length, jet velocity, and flap angle. It may be observed in this figure that the data collapse very well using these variables for different jet velocities, flow length, and flap angles.

The development of this empirical method for USB noise prediction is still in progress. However, the preliminary formulation using the data from small-scale model static tests with the jet flow at ambient temperature is given below.

$$S_N = \frac{f_c L_F}{V_J} \left[1 + \delta_f\right]^{1/3}$$

$$SPL(S_N) = 10 \log \left(\frac{V_J}{V_o}\right)^{n,(\theta'',\phi)} + 10 \log \frac{A_N}{A_o} - 20 \log \frac{R}{R_o}$$

$$- 10 \log \left[(AR_N)^{1/3} \frac{L_F}{D_H}\right] + K_1(\theta'') + k_2(\phi) \qquad (3)$$

where

S_N nondimensional frequency (Strouhal number)

f_c center frequency of one-third octave band

δ_f flap angle (radians)

$n(\theta'',\phi)$ velocity exponent as a function of direction, θ'' and ϕ (for definition of θ'' and ϕ see figure 12)

V_J	jet velocity (m/s)
V_o	reference velocity = 180 m/s
A_N	nozzle exit area (m^2)
A_o	reference nozzle area = 1 m^2
R	distance from nozzle to measurement location (m)
R_o	reference distance = 1 m
AR_N	aspect ratio of nozzle (width-to-height ratio)
D_H	hydraulic diameter of the nozzle exit (m)

The noise levels are calculated using equation (3) for small scale model and large scale model static cases. These results are compared with the measured data in figures 14 and 15. The agreement is very reasonable.

Until more data are available and analyzed, the effect of aircraft motion may be incorporated in the same way as given in reference 13. The preliminary indications of the recent data from Lockheed's Acoustic Free-Jet facility are that the spectral characteristics of sound change as the free-stream flow is introduced. The high-frequency noise does not reduce in the aft quadrant. The examination of the flow characteristics revealed that the jet flow separated from the surface just ahead of the trailing edge with the forward speed. Therefore, it is necessary to consider this aspect of the problem in analyzing and interpreting the data on the forward speed effect.

CONCLUDING REMARKS

An empirical noise prediction method has been developed using the extensive acoustic experimental data for USB configuration. The method is simple to use and correlates reasonably well with the available static test data. The effect of forward speed and the ground reflections for the case of aircraft in flight may be easily incorporated in the program.

It is conjectured from the experimental data that the noise generated in the vicinity of the trailing edge is a dominant source contributing to the radiated sound field in the direction below the wing. A mathematical model has been developed to predict the directivity and spectral distribution of the noise generated in the sheared layer of the trailing edge wake. These results are in good agreement with the experimentally measured data, which indicate the dominant noise is generated by the flow mixing where the velocity gradient is very large.

The results presented here indicate that one of the ways of reducing USB noise is to modify the shear layer and thus modify the turbulence generation in

the trailing edge wake. Accomplishment of this noise reduction requires more experimental and theoretical study.

More exploratory study is necessary to evaluate the flow characteristics in the trailing edge in order to correlate the relationship between the trailing edge flow and the geometric and operational parameters. This would yield a better analytical approach to predict the noise levels and also reveal the ways of controlling USB noise.

APPENDIX

SYMBOLS

Additional symbols used in the text and in figures are defined in this appendix.

AR	aspect ratio
C	chord
h	nozzle height
L_F	flow length
L_x	longitudinal length scale of eddy
L_y	spanwise length scale of eddy
R_c	flap radius of curvature
R_w	correlation function
$\bar{U}$	mean velocity
U_J	jet exit velocity
X	nozzle location
$\bar{x}$	separation distance
x'	streamwise location of first hot wire
x''	streamwise location of second hot wire
y'	spanwise location of first hot wire
y''	spanwise location of second hot wire
z'	lateral position of first hot wire
z''	lateral position of second hot wire
Θ	angle from forward axis of the jet in the flyover plane
Θ'	angle of the wing surface in the flyover plane
Θ''	angle from trailing edge surface in the flyover plane (see fig. 12)

Θ_N	nozzle impingement angle
ρ	density of the flow
ϕ	azimuthal angle (angle from the wing plane)

REFERENCES

1. Reddy, N. N.; and Brown, W. H.: Acoustic Characteristics of an Upper-Surface Blowing Concept of Power-Lift System. AIAA Paper 75-204, Jan. 1975.

2. Reddy, N. N.: Propulsive-Lift Noise of an Upper Surface Blown Flap Configuration. AIAA Paper 75-470, March 1975.

3. Von Glahn, U.; and Groesbeck, D.: Acoustics of Attached and Partially Attached Flow for Simplified OTW Configurations with 5:1 Slot Nozzle. NASA TMX-71807, Nov. 1975.

4. Hayden, R. E.: Sound Generation by Turbulent Wall Jet Flow Over a Trailing Edge. M.S. Thesis, Purdue University, 1969.

5. Ffowcs Williams, J. E.; and Hall, L. H.: Aerodynamic Sound Generated by Turbulent Flow in the Vicinity of Scattering Half Plane. *J. Fluid Mech.*, vol. 40, pt. 4, 1970, pp. 657-670.

6. Siddon, T. E.: Surface Dipole Strength by Cross-Correlation Method. *J. Acous. Soc. Am.*, vol. 53, no. 2, 1973.

7. Brown, W. H.; and Reddy, N. N.: USB Flow Characteristics Related to Noise Generation. Powered-Lift Aerodynamics and Acoustics, NASA SP-406, 1976. (Paper no. 14 of this compilation.)

8. Gibson, J. S; and Searle, N.: Characteristics of USB Noise. Powered-Lift Aerodynamics and Acoustics, NASA SP-406, 1976. (Paper no. 15 of this compilation.)

9. Olsen, W. A.; Dorsch, R. G.; Miles, J. H.: Noise Produced by a Small-Scale, Externally Blown Flap. NASA TN D-6636, March 1972.

10. Maestrello, L.: Measurement and Analysis of the Response Field of Turbulent Boundary Layer Excited Panels. *J. Sound Vib.*, vol. 2, no. 3, 1965.

11. Maestrello, L.: Use of Turbulent Model to Calculate the Vibration and Radiation Responses of a Panel With Practical Suggestions for Reducing Sound Level. *J. Sound Vib.*, vol. 5, no. 3, 1967.

12. Tam, C. K. W.: Intensity, Spectrum, and Directivity of Turbulent Boundary Layer Noise. *J. Acous. Soc. Am.*, vol. 57, 1975, pp. 25-34.

13. Tam, C. K. W.; and Reddy, N. N.: Sound Generated in the Vicinity of Trailing Edge of an Upper Surface Blown Flap. AIAA Paper No. 76-503, July 1976.

14. Dorsch, R. B.; Clark, B. J.; and Reshotko, M.: Interim Prediction Method for Externally Blown Flap Noise. NASA TM X-71768, 1975.

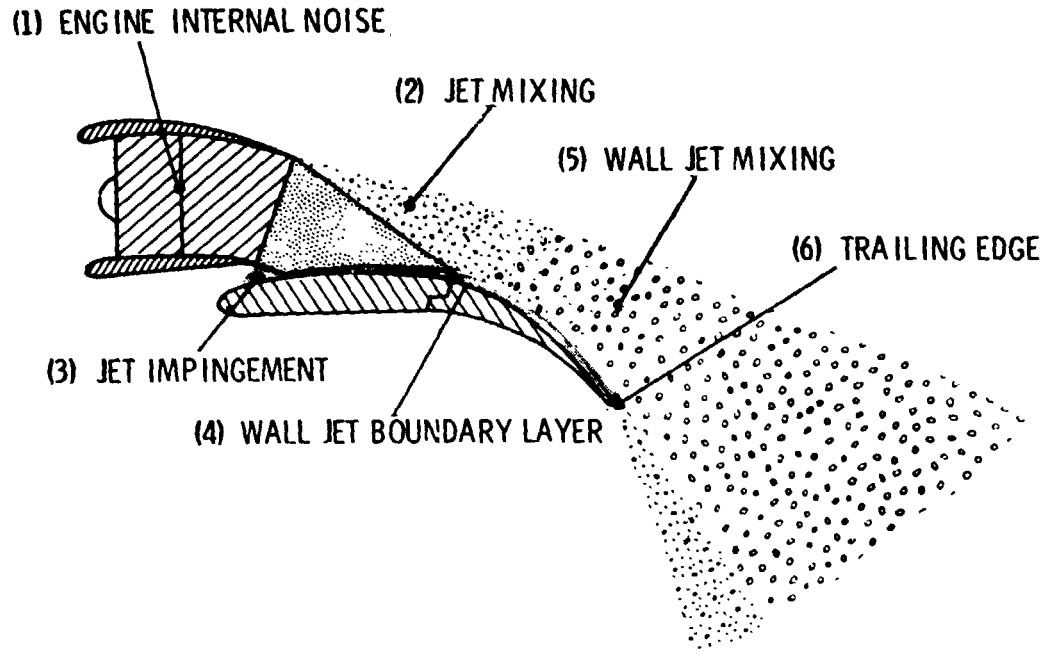

Figure 1.- USB noise source mechanisms.

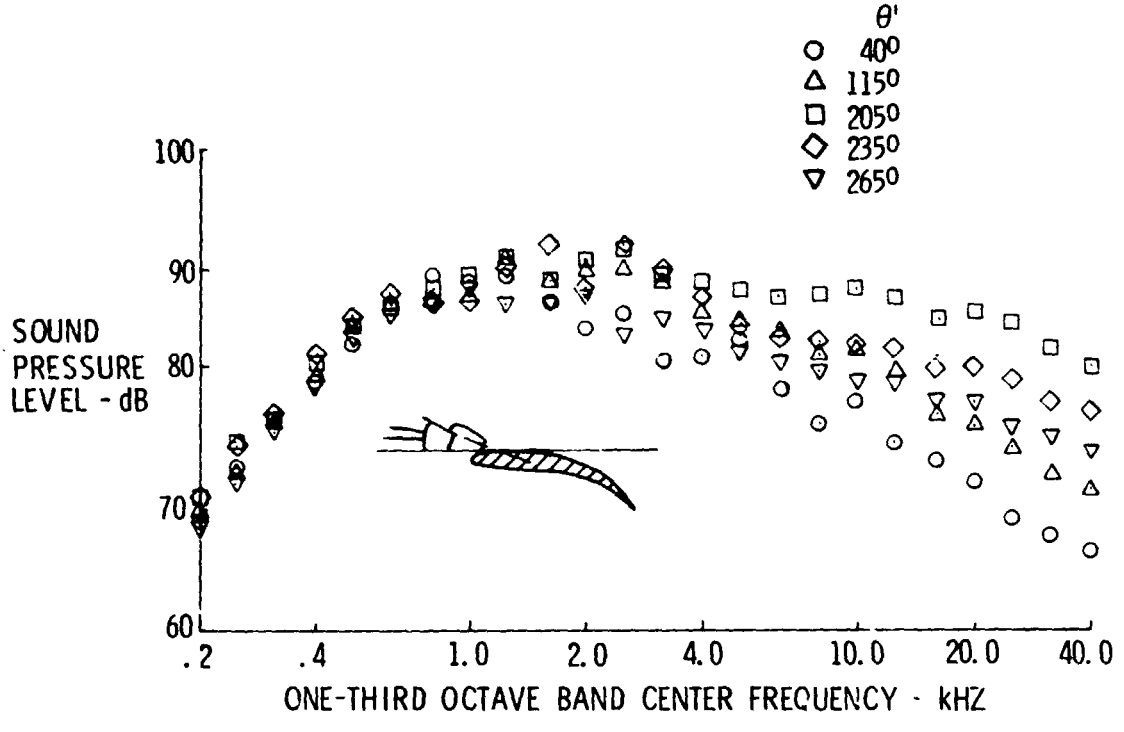

Figure 2.- Typical spectral distribution as a function of various angles in the flyover plane.

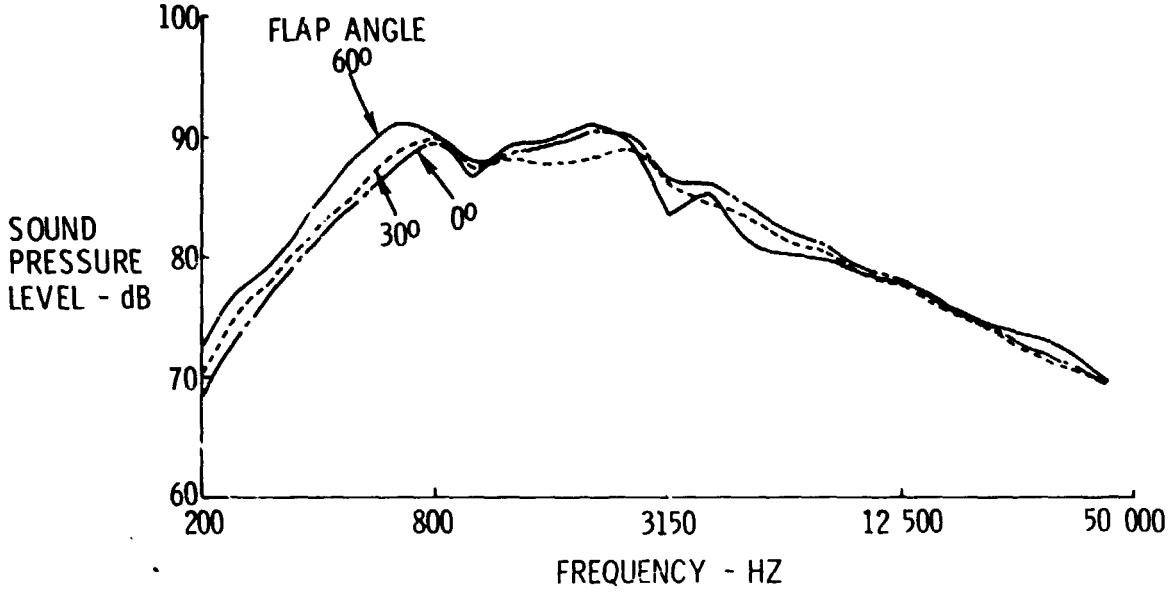

Figure 3.- Effect of flap angle on sound spectrum in flyover plane. $\Theta = 90^{\circ}$; $R_c = 7.62$ cm; $L_F = 22.66$ cm; $V_J = 215$ m/s; AR of nozzle = 4; X = 20% C; $\Theta_N = 20^{\circ}$.

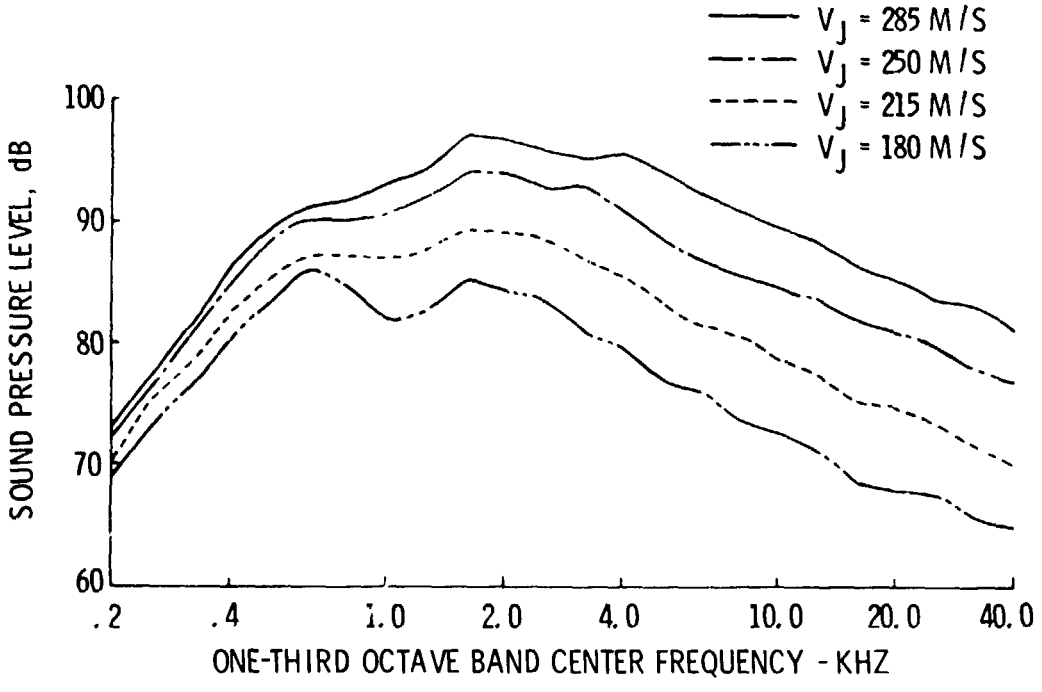

Figure 4.- Effect of jet velocity on spectral distribution in flyover plane. $\Theta = 90^{\circ}$; $R_c = 7.62$ cm; $L_F = 22.66$ cm; AR of nozzle = 4; X = 20% C; $\Theta_N = 20^{\circ}$.

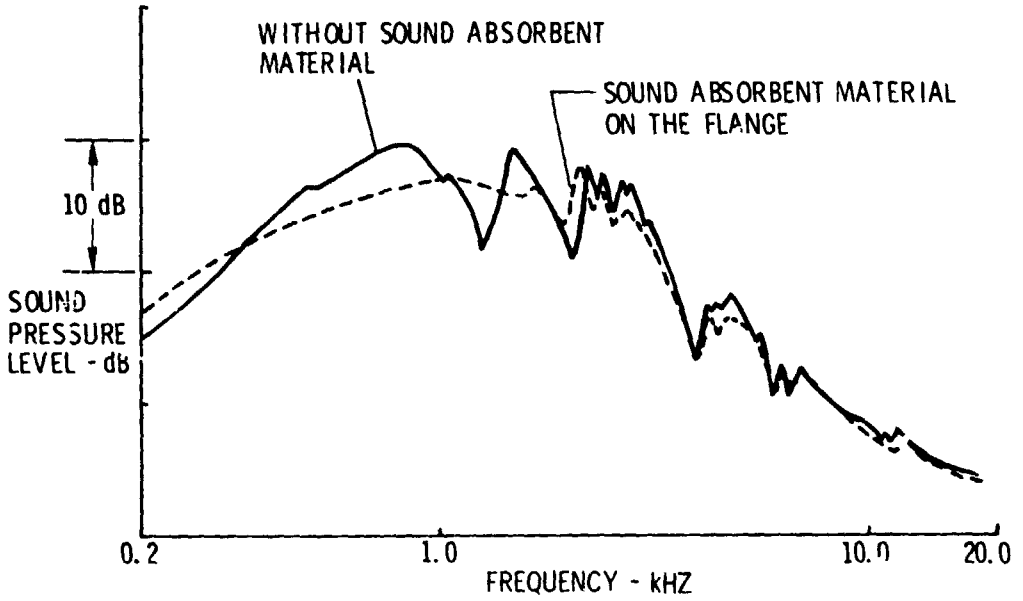

Figure 5.- Effect of nozzle surface diffraction on radiated sound in narrow-band analysis. $\Theta = 90^{o}$; $R_c = 7.62$ cm; $L_F = 22.66$ cm; AR of nozzle = 4; X = 20% C; $\Theta_N = 20^{o}$; $V_J = 215$ m/s.

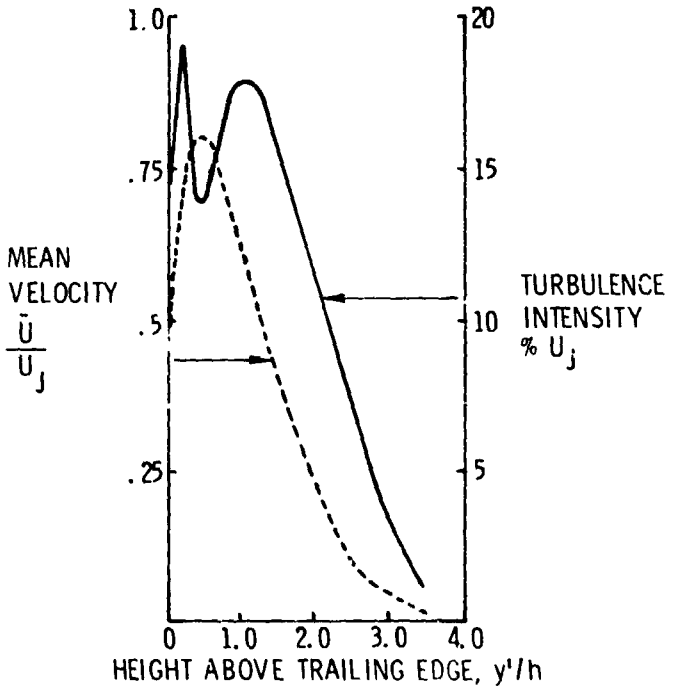

Figure 6.- Typical velocity and turbulence intensity profiles just downstream of trailing edge.

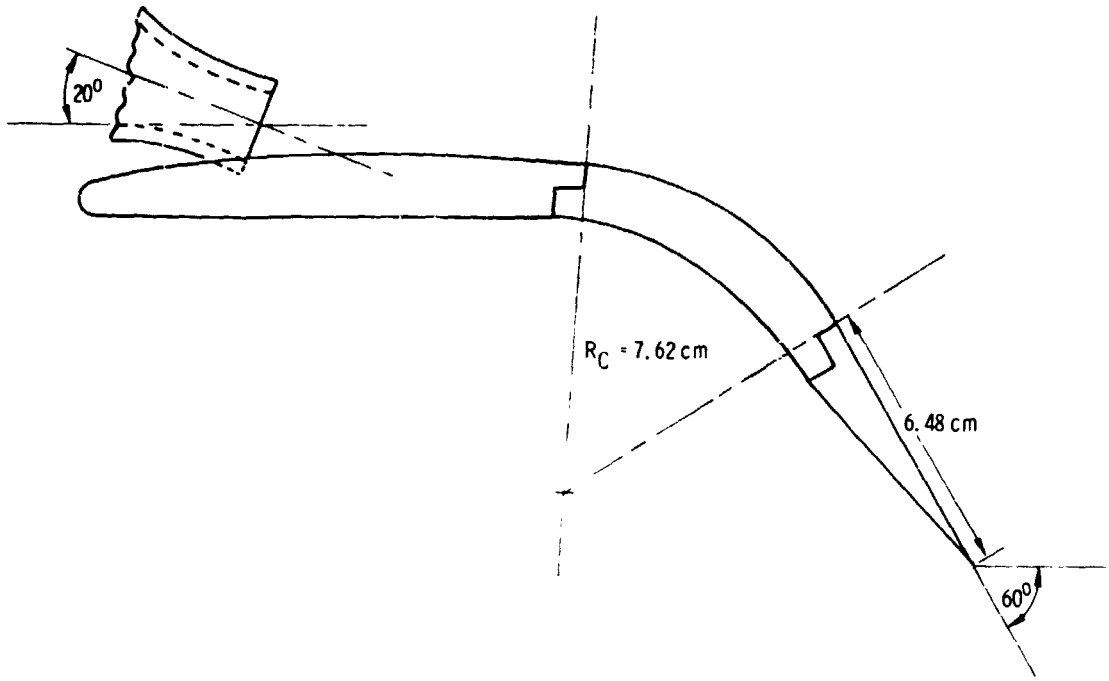

Figure 7.- Typical streamwise space-time cross correlations in the trailing edge wake.

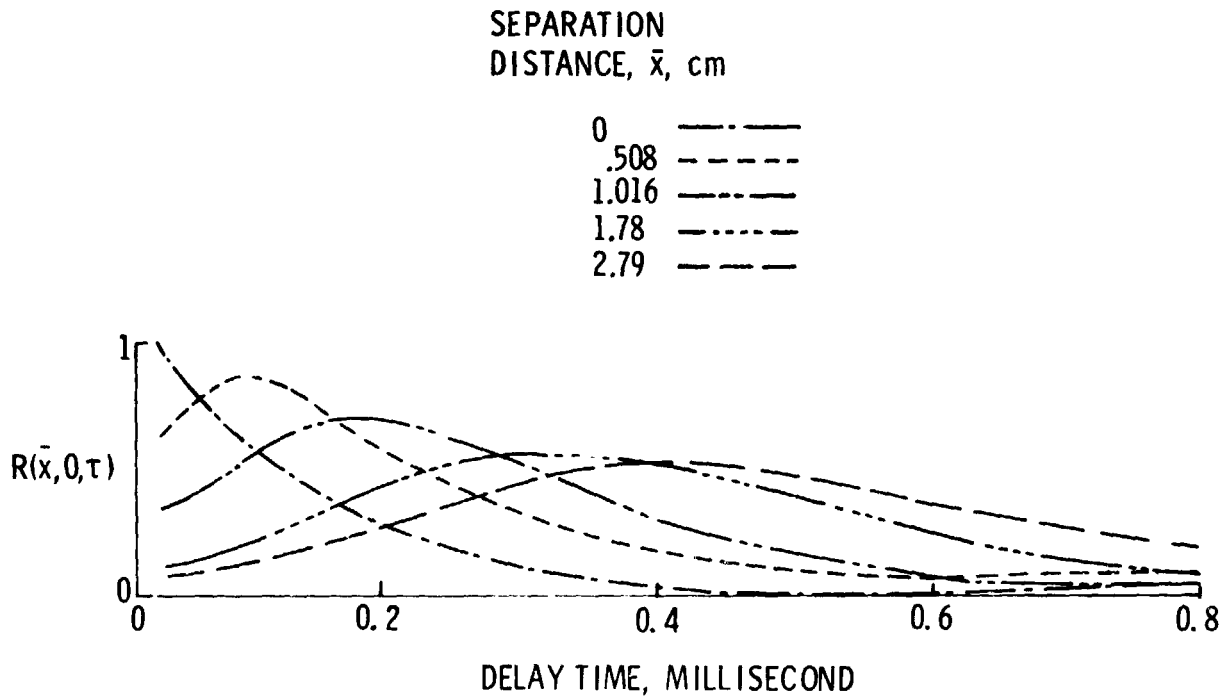

Figure 8.- USB configuration used for flow measurements.

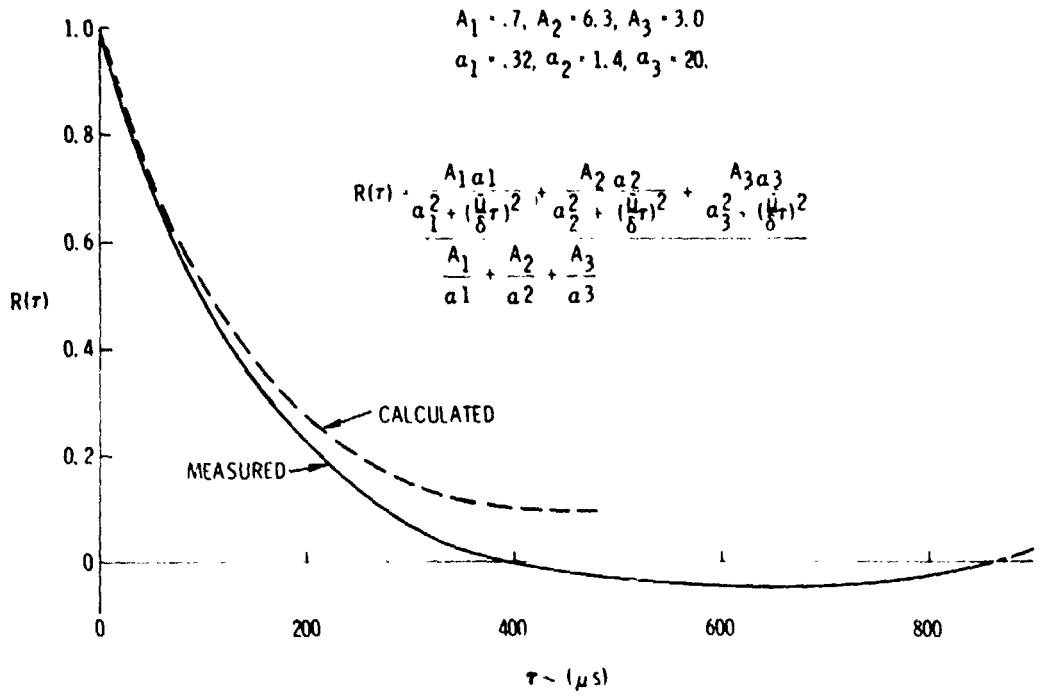

Figure 9.- Autocorrelation function of turbulence just downstream of trailing edge.

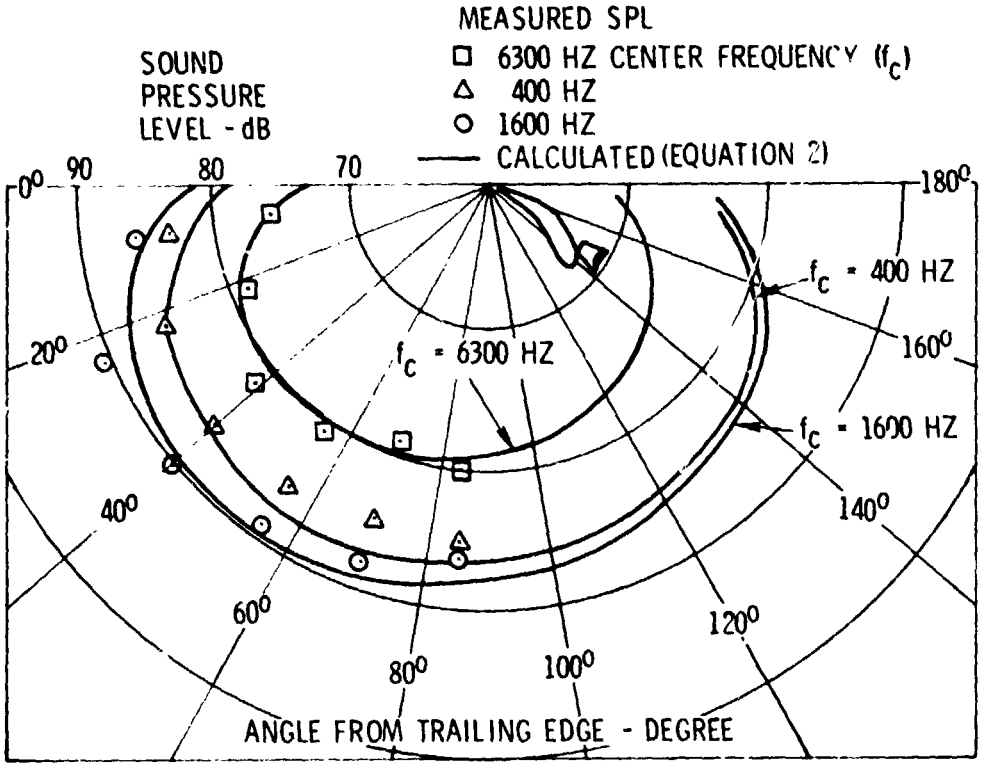

Figure 10.- Comparison between calculated and measured sound.

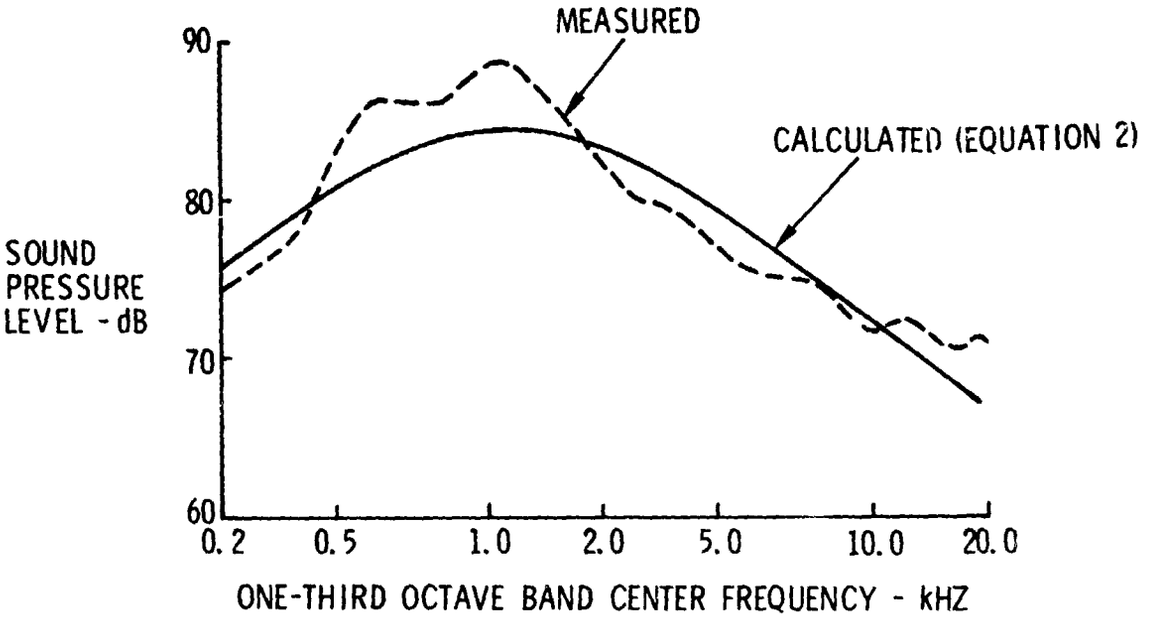

Figure 11.- Comparison between calculated and measured spectra.

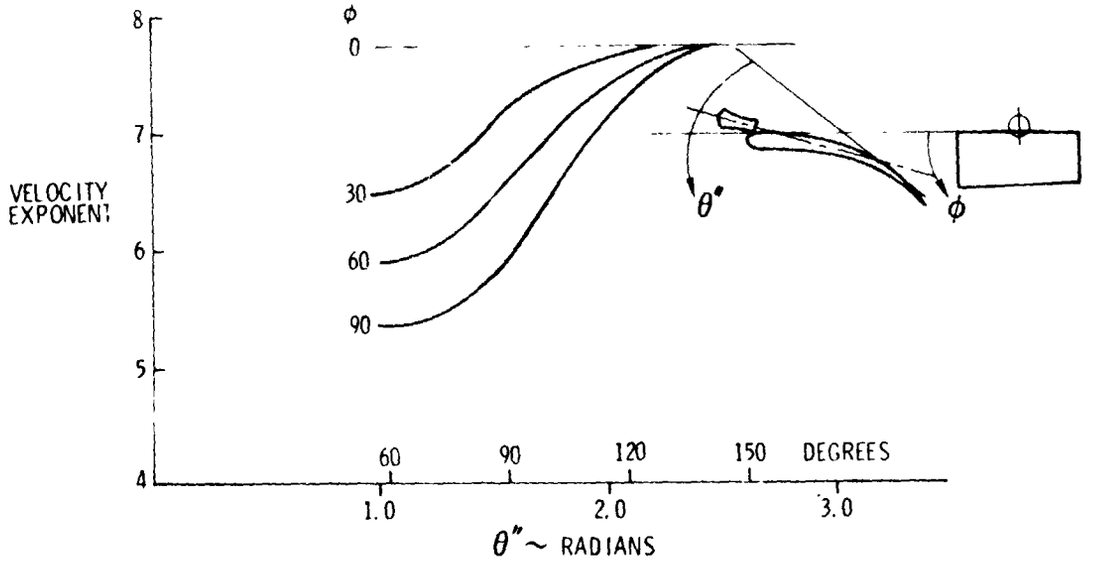

Figure 12.- Velocity exponent for USB noise.

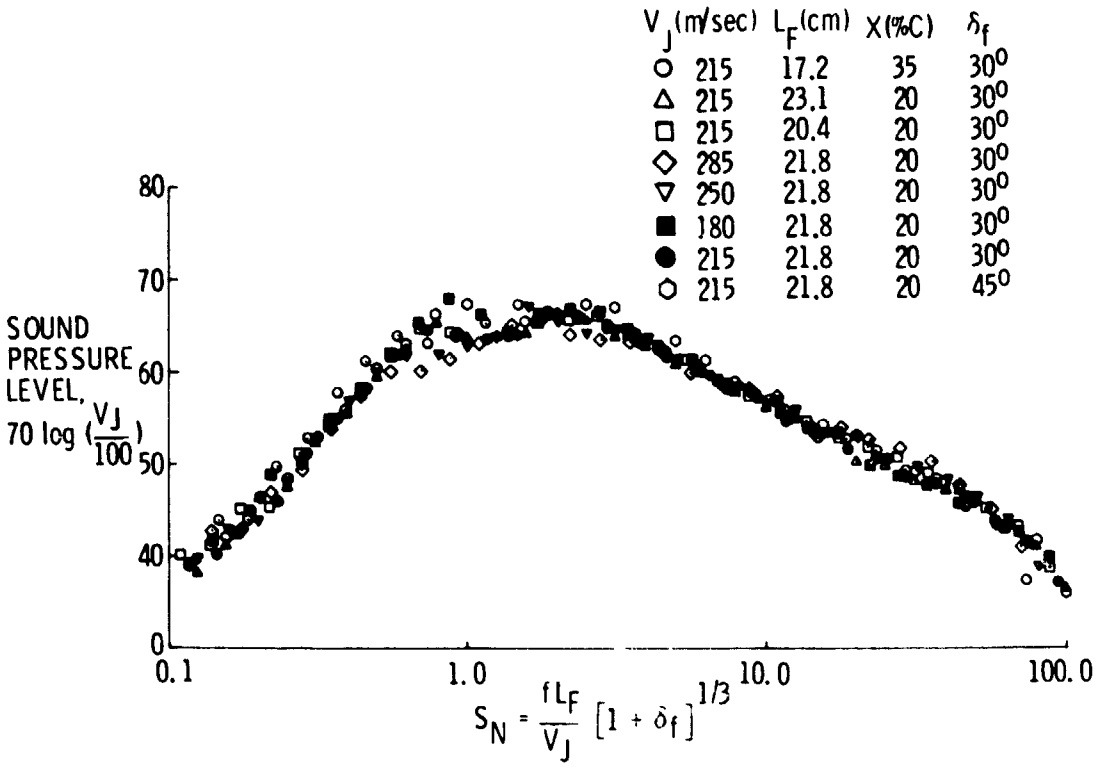

Figure 13.- Normalized spectra for USB noise. $\Theta'' = 115^\circ$.

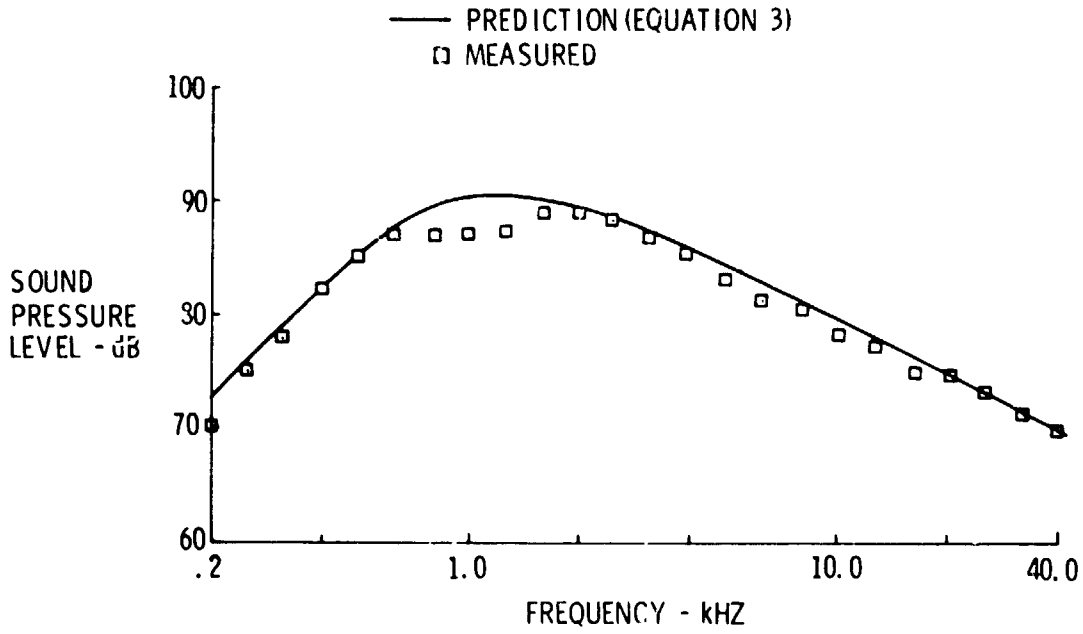

Figure 14.- Comparison of empirical prediction with experimental data in flyover plane. $A_N = 20.25$ cm^2; AR of nozzle = 4; $\delta_f = 30^\circ$; $\Theta = 85^\circ$.

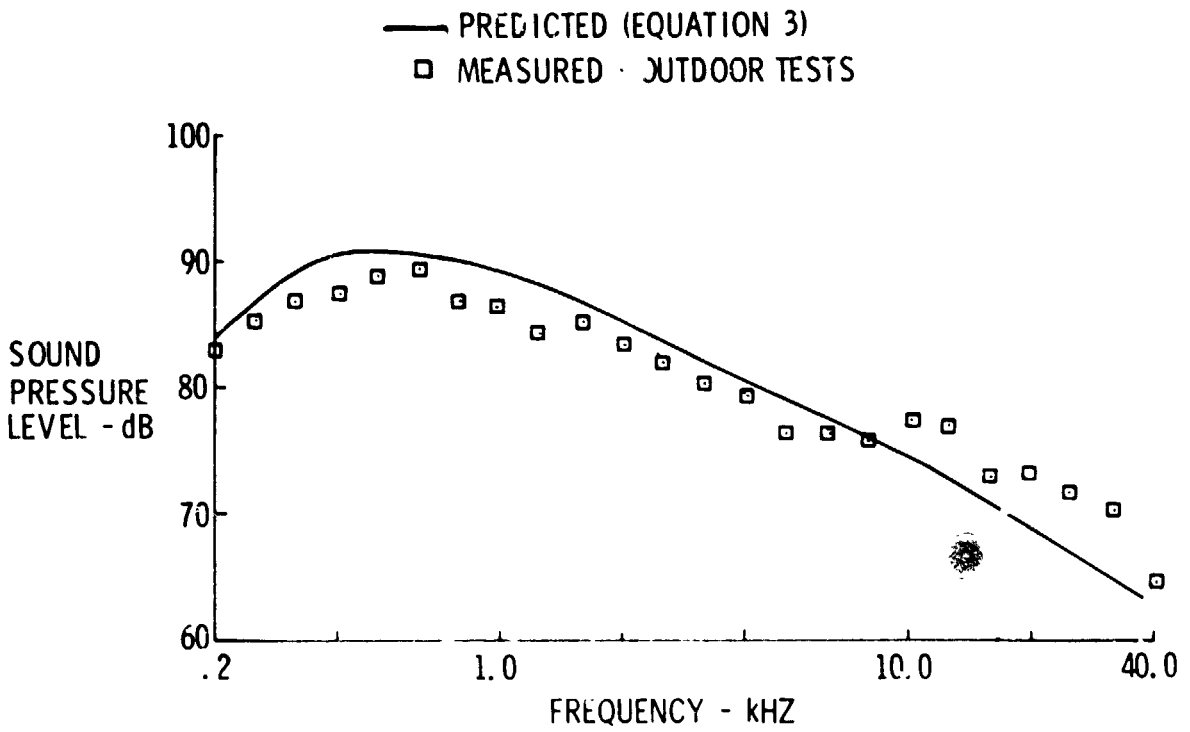

Figure 15.- Comparison of empirical prediction with experimental data in flyover plane. A_N = 113.8 cm^2; AR of nozzle = 4; $\delta_f = 30^\circ$; $\Theta = 130^\circ$.